

The algorithm for the FAST reconstruction and its performance

PhD thesis Justin Albury

<https://digital.library.adelaide.edu.au/dspace/handle/2440/130770>

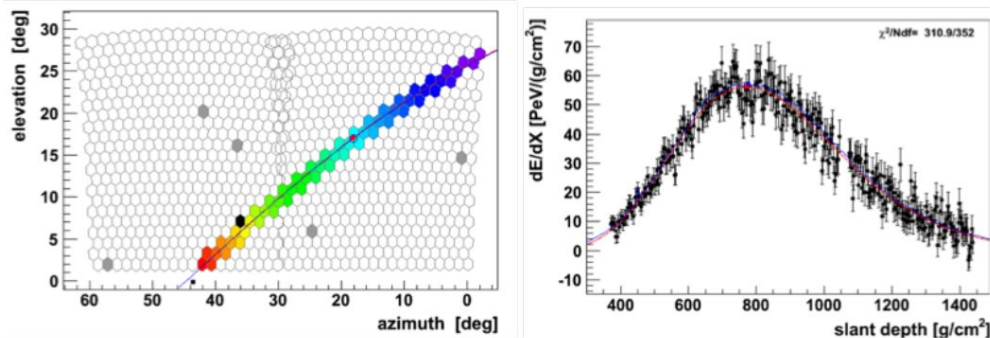


Jose Bellido

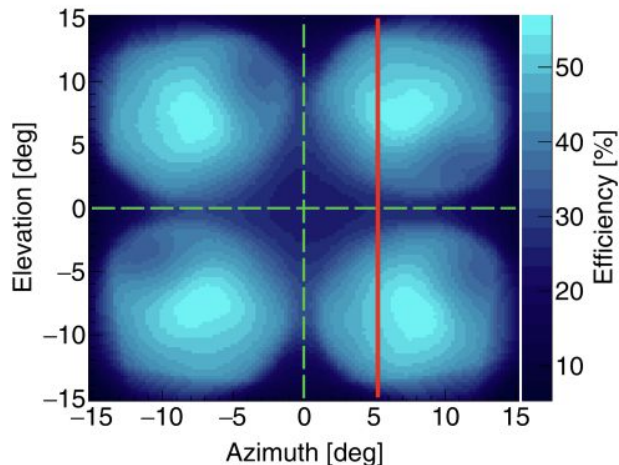
GCOS workshop 2022

Wuppertal 13 - 15 July 2022

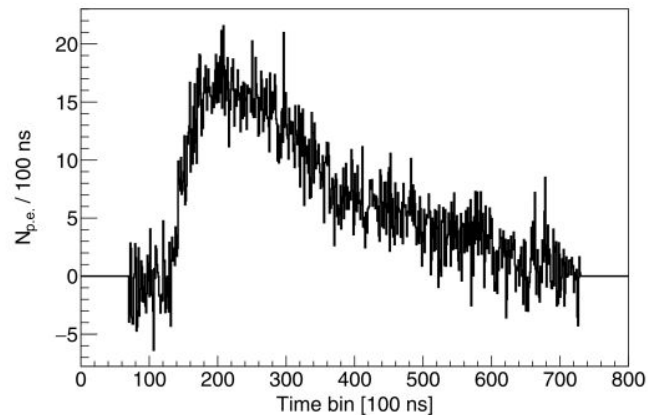
Pierre Auger: Traditional reconstruction of the shower (i.e. Geometry and then shower profile)



FAST: Both, Geometry and shower profile (i.e Xmax and Energy) need to be estimated from the pulse information.



(a)



(b)

Figure 6.5. (a) The path of the CLF at TA (red) across the FoV of the FAST camera and (b) an example detection of the CLF (an average of 200 laser shots) with the central FAST telescope [217].

Shower Reconstruction with a FAST Array

(Long story short)

A learning machine algorithm is used to find a first guess of the shower parameters

A learning machine algorithm is used to obtain a first guess of the shower reconstruction (i.e. geometry, Xmax and Energy).

Training sample: 500,000 events simulated within a small core region of 1 km of radius, 80% for training and 20% for validation.

Input parameters: centroid time, total signal, pulse height

Resolution and Bias

Shower axis: Res. $\sim 2.76^\circ$, Bias $< 0.75^\circ$

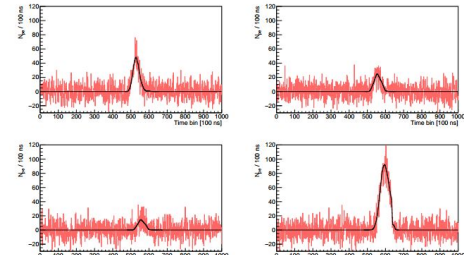
Core: Res. $\sim 256\text{m}$, Bias $< 50\text{m}$

Xmax: Res. $\sim 60\text{ g/cm}^2$, Bias $< 30\text{ g/cm}^2$

Energy: Res. $\sim 25\%$, Bias $< 15\%$

A given atmosphere model is used for training. So, no atmosphere measurements are considered.

A Top Down reconstruction (inverse MC) algorithm is used to fine tune the shower reconstruction



Parameter	Simulated Value	First Guess	Reconstructed Value
X_{max} [g/cm^2]	750	750	751.8 ± 9.6
Energy [EeV]	31.6	31.6	31.2 ± 0.7
Zenith [deg]	30	30	31.2 ± 0.3
Azimuth [deg]	50	50	49.8 ± 0.8
CoreX [m]	500	500	516.0 ± 45.6
CoreY [m]	-500	-500	-515.9 ± 34.4

Parameter	Simulated Value	First Guess	Reconstructed Value
X_{max} [g/cm^2]	750	700	754.2 ± 9.9
Energy [EeV]	31.6	30	31.3 ± 0.7
Zenith [deg]	30	30.5	29.2 ± 0.1
Azimuth [deg]	50	53	50.4 ± 1.0
CoreX [m]	500	550	455.1 ± 7.1
CoreY [m]	-500	-350	-478.8 ± 36.7

learning machine algorithm performance

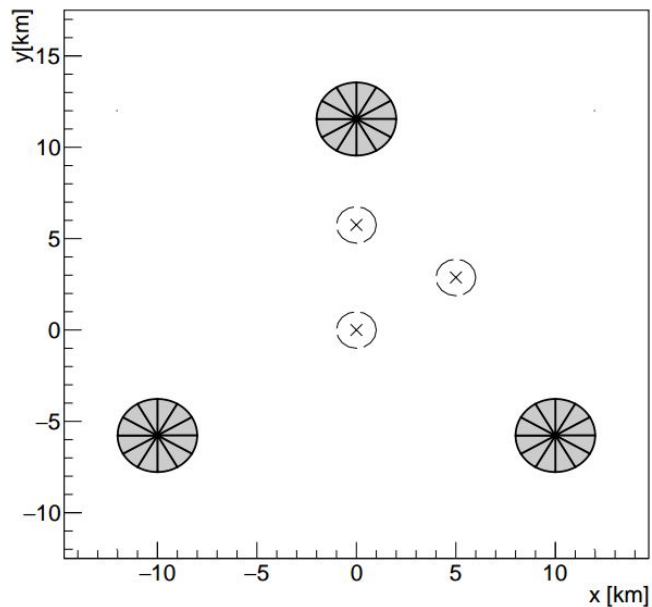
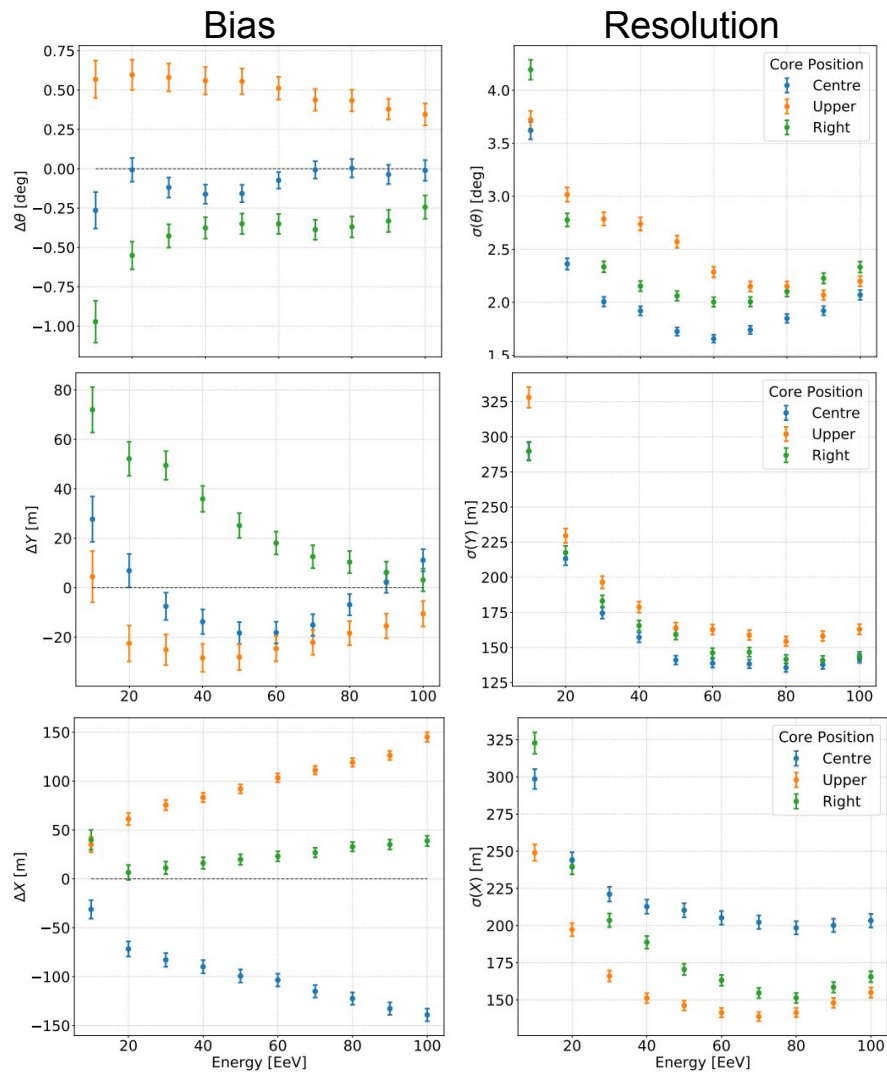


Figure 8.2. The configuration of the simulated FAST stations used for the training and testing of the neural network reconstruction. The dashed lines represent the regions within which core positions of the simulated showers are sampled uniformly, and the crosses represent their centres.



learning machine algorithm performance

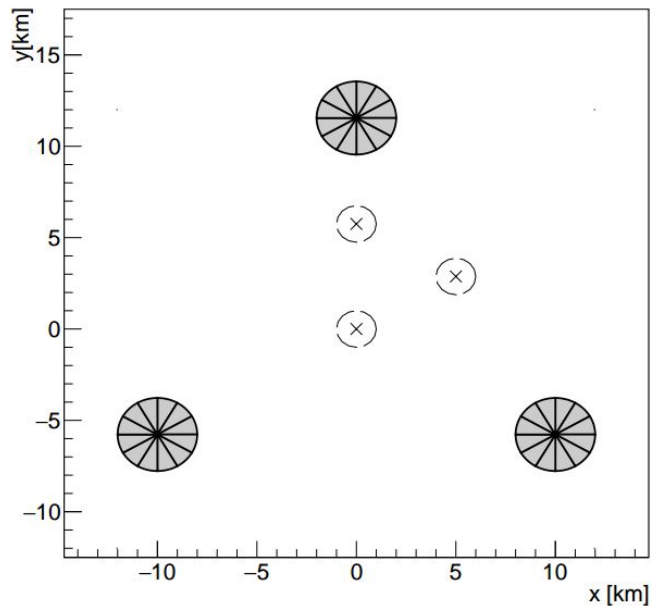
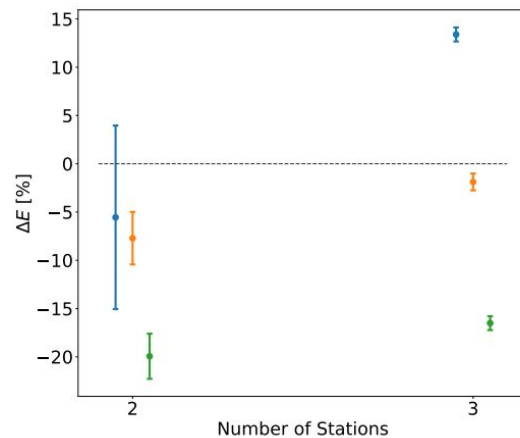
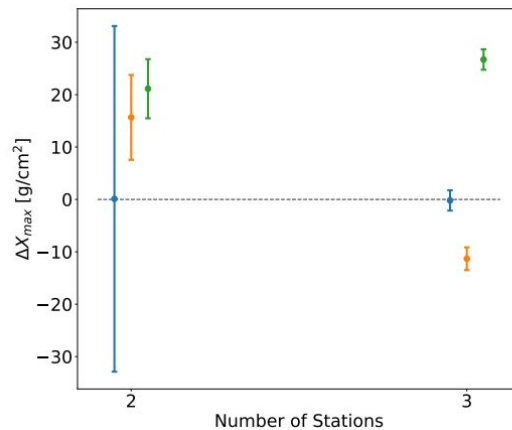
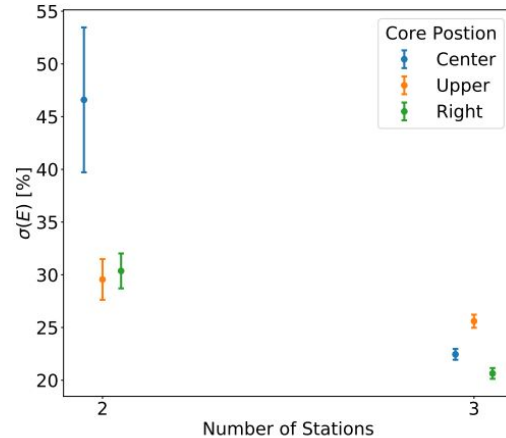
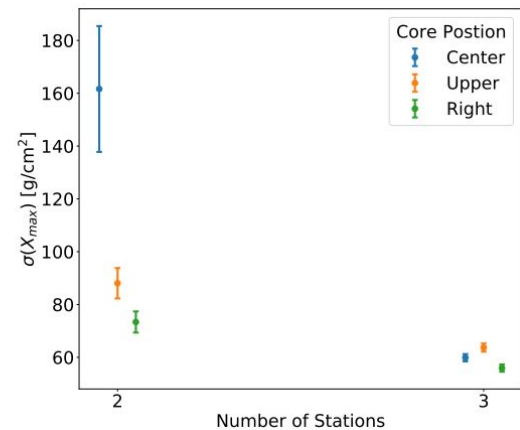


Figure 8.2. The configuration of the simulated FAST stations used for the training and testing of the neural network reconstruction. The dashed lines represent the regions within which core positions of the simulated showers are sampled uniformly, and the crosses represent their centres.

Bias



Resolution



Impact of systematic in the telescope pointing directions

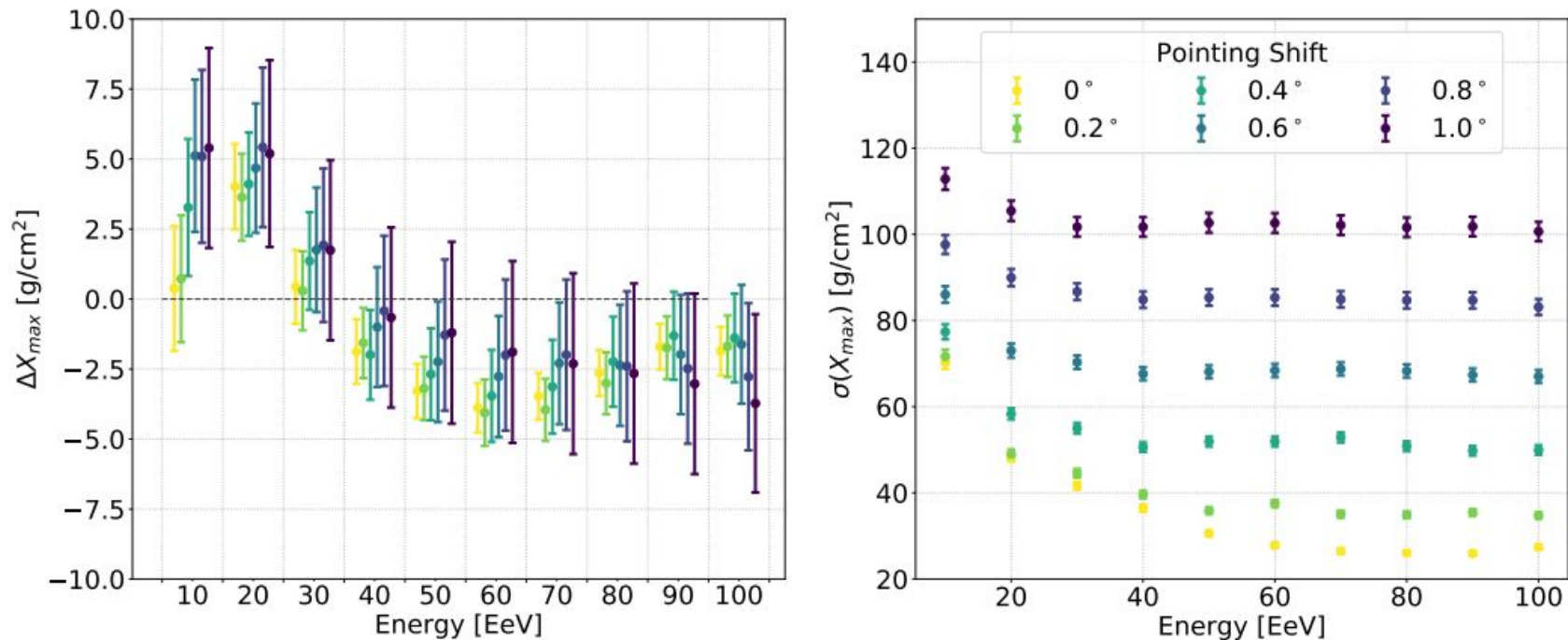


Figure 8.25. The X_{\max} bias (left) and resolution (right) as a function of energy for the central core position shown in Figure 8.2 with modified telescope pointing directions. The data points in the left panel are shifted laterally to aid the reader. The grid lines separate each energy bin.

Impact of systematic in the atmospheric parameters

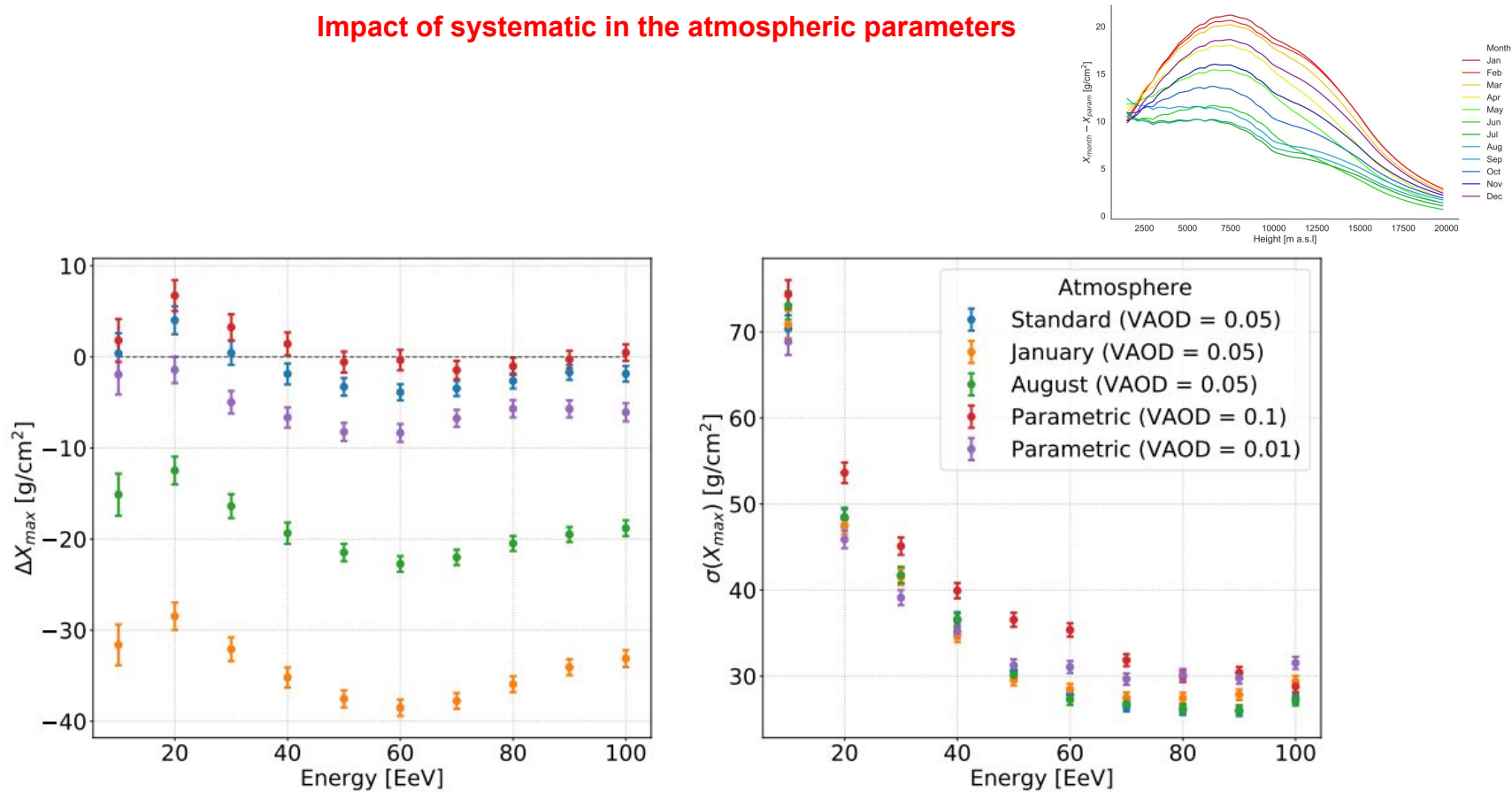


Figure 8.31. The X_{max} bias (left) and resolution (right) as a function of energy for the central core position shown in Figure 8.2 with modified atmospheric models.

Impact of systematic in the atmospheric parameters

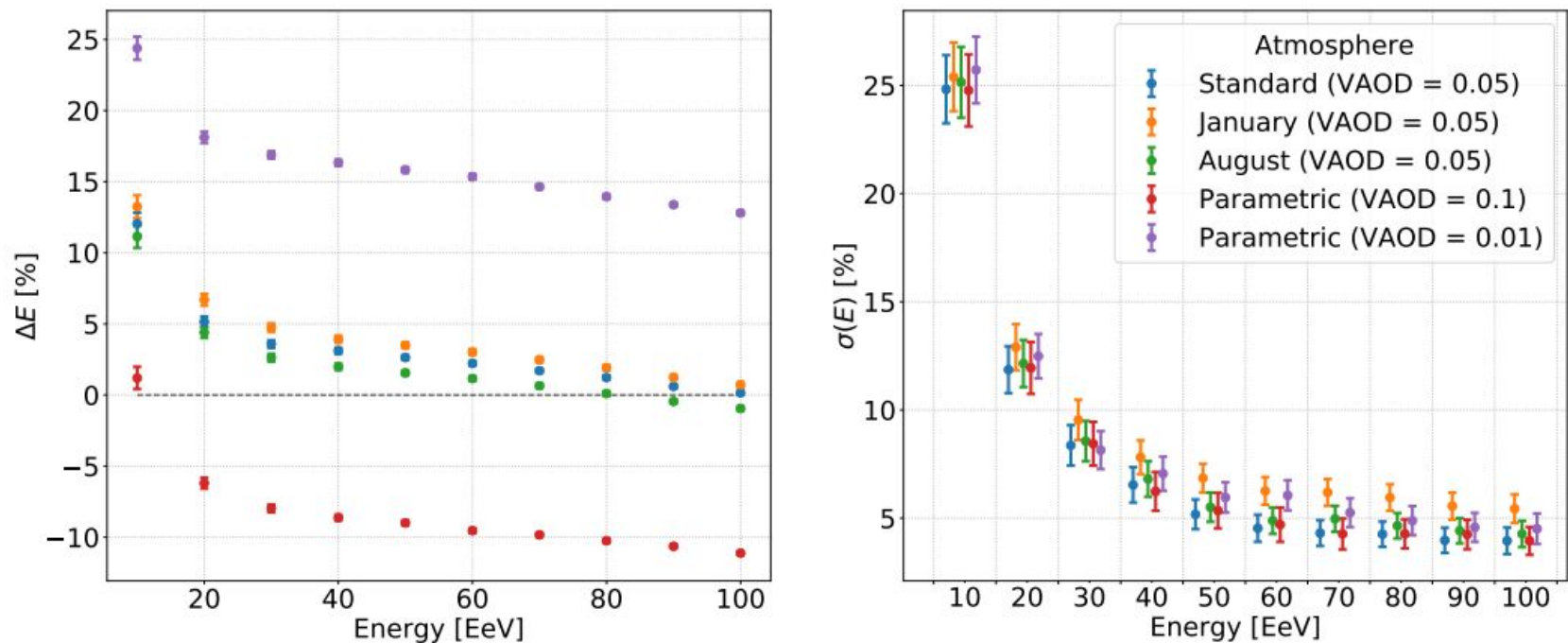
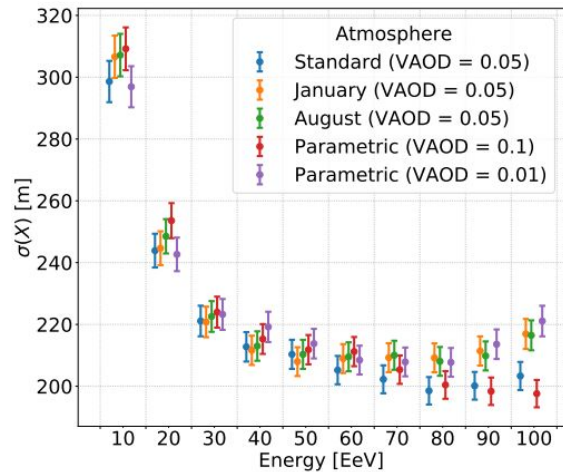
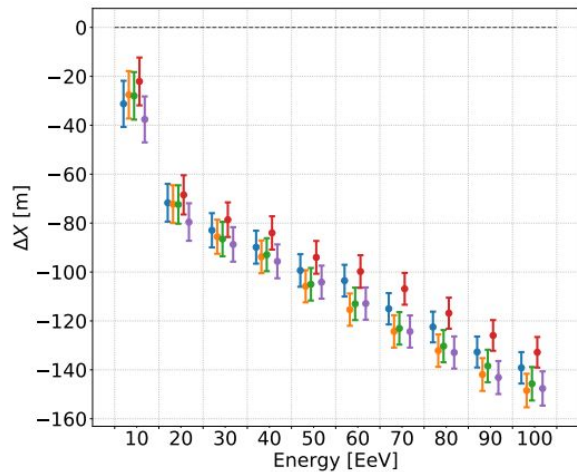
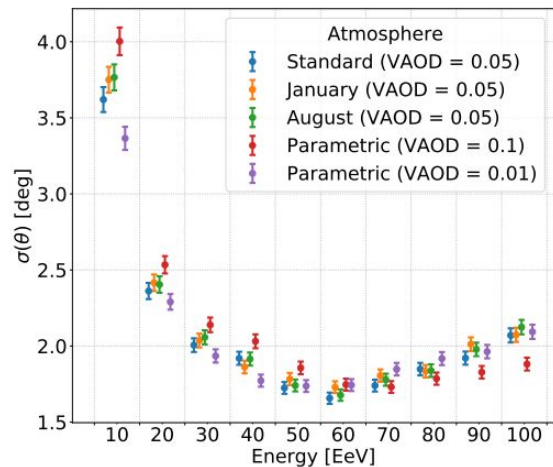
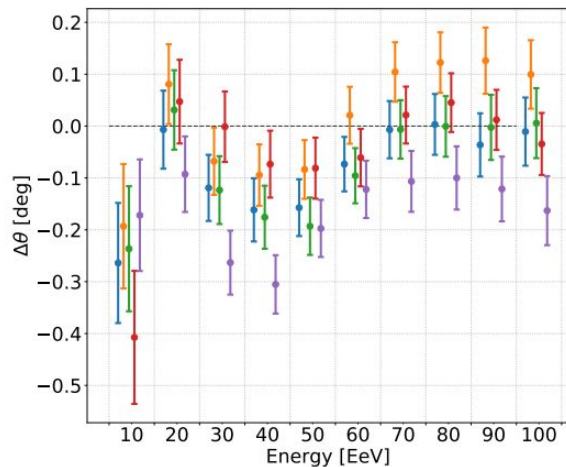


Figure 8.33. The energy bias (left) and resolution (right) as a function of energy for the central core position shown in Figure 8.2 with modified atmospheric models. The data points in the right panel are shifted laterally to aid the reader. The grid lines separate each energy bin.

Impact of systematic in the atmospheric parameters



Top Down Reconstruction Performance Test

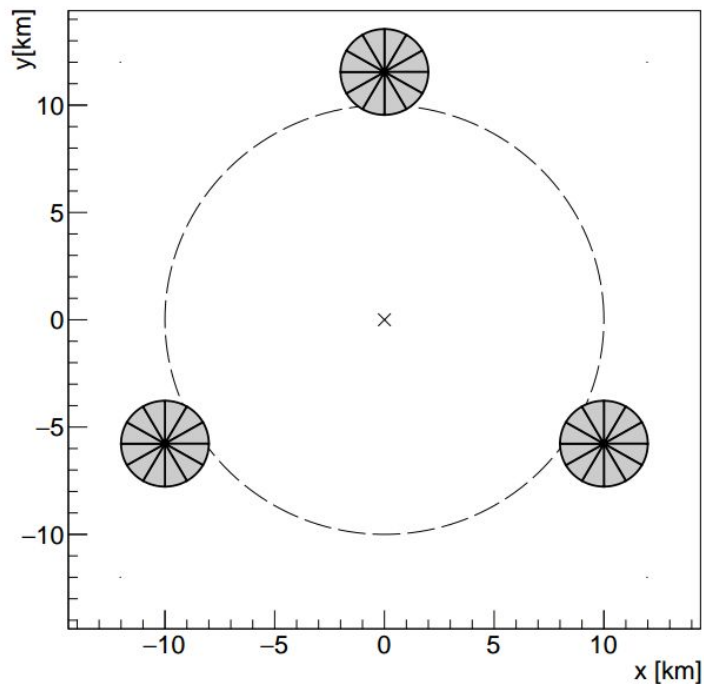


Figure 7.7. The configuration of the simulated FAST stations. The dashed line represents the region within which core positions of simulated showers are sampled uniformly, and the cross represents the centre of the cell.

Reconstructing X_{\max} only

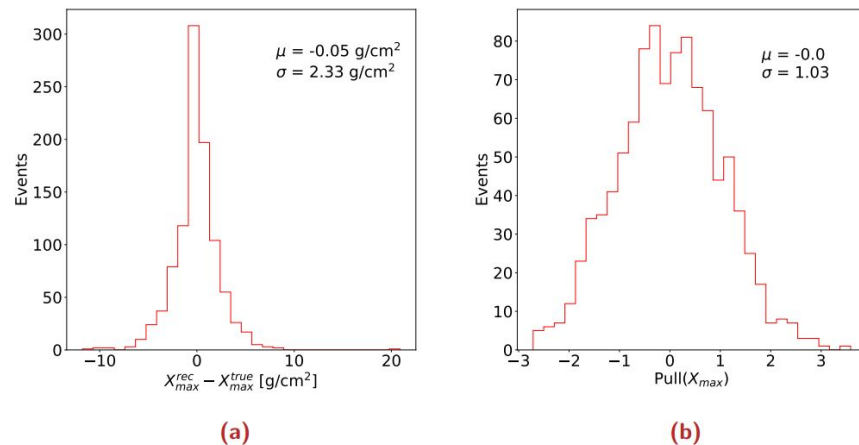


Figure 7.9. Distributions of (a) the difference between simulated and reconstructed X_{\max} and (b) the X_{\max} pull distribution. Note the means are close to 0 and the pull distribution is very close to a standard normal distribution (mean 0 and variance 1) indicating that the associated uncertainties in X_{\max} are consistent with the random fluctuations in the reconstructed value of X_{\max} .

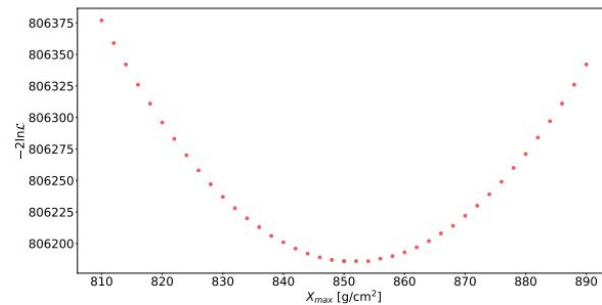


Figure 7.8. The negative log-likelihood ($-2 \ln \mathcal{L}$) plotted as a function of X_{\max} . Note that the minimum corresponds to the reconstructed X_{\max} of $\sim 852 \text{ g/cm}^2$.

Top Down Reconstruction Performance Test

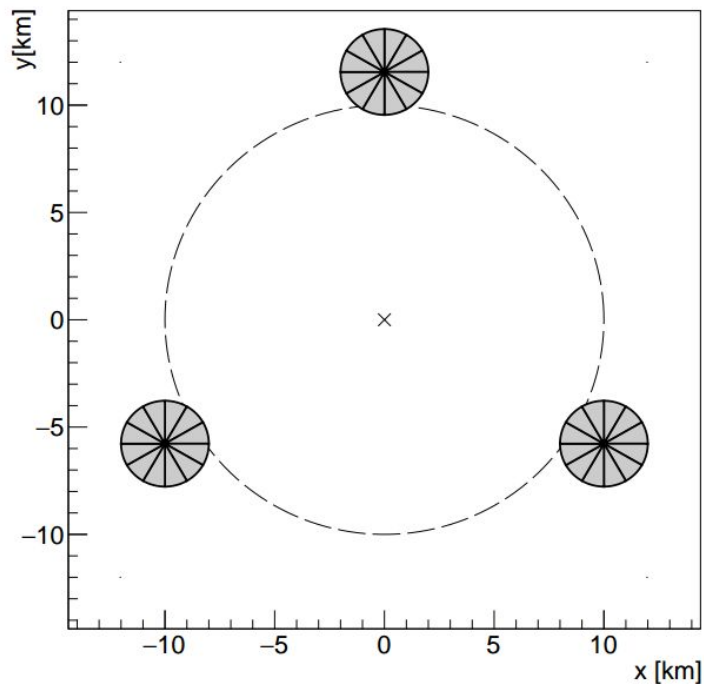


Figure 7.7. The configuration of the simulated FAST stations. The dashed line represents the region within which core positions of simulated showers are sampled uniformly, and the cross represents the centre of the cell.

Reconstructing Energy only

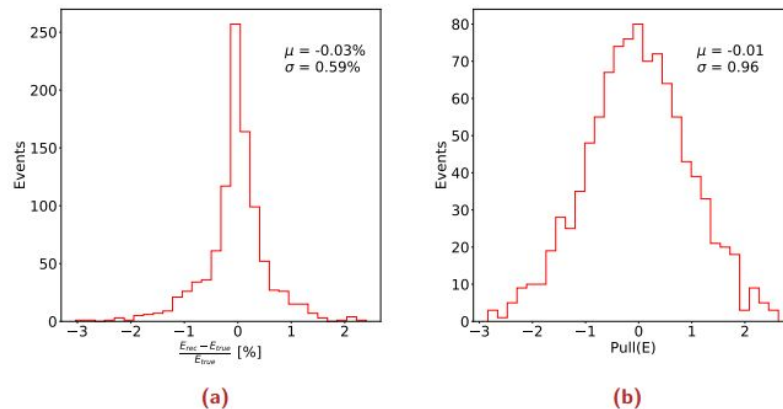


Figure 7.11. Distributions of (a) the relative difference between simulated and reconstructed energy and (b) the energy pull distribution. Note the means are close to 0 and the pull distribution is very close to a standard normal distribution (mean 0 and variance 1) indicating that the associated uncertainties in energy are consistent with the random fluctuations in the reconstructed value of energy.

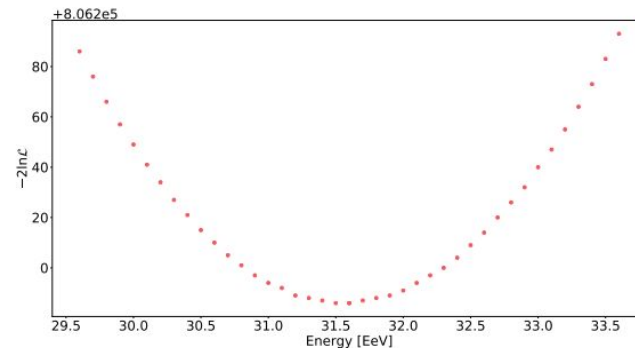


Figure 7.10. The negative log-likelihood ($-2 \ln \mathcal{L}$) plotted as a function of energy.

7.4 Reconstruction Algorithm

The reconstruction software `FAST-rec` is implemented in C++ using the FAST modified version of the Auger Offline software framework described in Section 7.3. The author has developed all reconstruction software, including a new event structure which utilises the ROOT file format. A description of this FAST event structure is provided in Appendix B to compliment the work presented in this chapter. An example sequence file for the reconstruction of FAST events is shown in Code 7.2.

```
1  <!-- A sequence for FAST shower reconstruction -->
2  <sequenceFile>
3    <enableTiming/>
4    <moduleControl>
5
6      <loop numTimes="unbounded" pushEventToStack="yes">
7
8        <module> FASTEventFileReaderUA      </module>
9        <module> FASTTopDownReconstructorUA </module>
10       <module> FASTEventFileExporterUA    </module>
11
12     </loop>
13
14   </moduleControl>
15 </sequenceFile>
```

Code 7.2 An example sequence file for the reconstruction of FAST events.